Inhibition of Proliferation and Differentiation of Mesenchymal Stem Cells by Carboxylated Carbon Nanotubes

Dandan Liu,[†,‡,⊥] Changqing Yi,[†,§,⊥] Dawei Zhang,[†] Jinchao Zhang,[‡,*] and Mengsu Yang[†,§,*]

[†]Key Laboratory of Biochip Technology, Biotech and Health Centre, Shenzhen Research Institute of City University of Hong Kong, Shenzhen, China, [‡]College of Chemistry and Environmental Science, Hebei University, Baoding, China, and [§]Department of Biology and Chemistry, City University of Hong Kong, Hong Kong, China. [⊥]These authors contributed equally to this work.

Multipotent mesenchymal stem cells (MSCs) have attracted particular attention in stem cell therapy and tissue engineering because they can be readily isolated and expanded *ex vivo* and induced either *in vitro* or *in vivo* to terminally differentiate into osteoblasts, chondrocytes, adipocytes, tenoctyes, and neural cells.[1−3] In parallel, developments of nanotechnology in the past few years have demonstrated great potential for the application of carbon nanotubes (CNTs) in biosensors, tissue engineering, and biomedical devices due to their unique electronic, chemical, and mechanical properties.[4−7] When CNTs are employed as biomaterials such as implants for fracture and scaffolds for bone tissue regeneration, where they are in direct contact with the bone, the reaction of the MSCs to CNTs is critical for functional maintenance of the biomaterials over time in the tissues.[8] However, the potential effect of CNTs on stem cell response and the mechanisms of stem cell−nanomaterial interactions are not well-understood.[9,10]

Osteoblasts and adipocytes all originate from MSCs and can transform mutually. There is a reciprocal relationship between the differentiation of adipocytic and osteogenic cells in MSC culture. An ideal bone regenerative material would inhibit adipocytic differentiation of MSCs and promote the production of mature osteoblasts. Since water-soluble CNTs will likely be used in biomedical applications, their cellular effects on MSC proliferation and differentiation and the associated molecular mechanisms were investigated in this study. We reported that carboxylated single-walled carbon nanotubes (SWCNTs) and carboxylated multiwalled carbon nanotubes (MWCNTs) inhibited the proliferation, osteogenic differentiation, adipogenic differentiation, and mineralization of MSCs. Oxidative stress assay indicated that reactive oxygen species (ROS) may not be responsible for the observed cytotoxicity of carboxylated CNTs. Quantitative polymerase chain reaction (Q-PCR) results and Western blot analysis together provided evidence that the inhibition of proliferation and osteogenic differentiation of MSCs may be modulated through a Smad-dependent bone morphogenetic protein (BMP) signaling pathway.

ABSTRACT Multipotent mesenchymal stem cells (MSCs) have attracted substantial attention in stem cell therapy and tissue engineering due to their ability to be cultured for successive passages and multilineage differentiation. Carbon nanotubes (CNTs) have been proposed to be used as potential biomedical structures for bone formation. Therefore, it is important to study the mechanisms of interaction between MSCs and CNTs. We demonstrated that carboxylated single-walled carbon nanotubes (SWCNTs) and carboxylated multiwalled carbon nanotubes (MWCNTs) inhibited the proliferation, osteogenic differentiation, adipogenic differentiation, and mineralization of MSCs. Oxidative stress assay indicated that reactive oxygen species (ROS) may not be responsible for the observed cytotoxicity of carboxylated CNTs. Quantitative real-time polymerase chain reaction (Q-PCR) experiments confirmed that the expression of osteoblast specific genes and adipocyte differentiation specific genes was greatly attenuated during the differentiation of MSCs in the presence of carboxylated CNTs. TEM images revealed that CNTs might interact with proteins located on the cell membrane or in the cytoplasm, which have a further impact on subsequent cellular signaling pathways. Q-PCR results and Western blot analysis together verified that the inhibition of proliferation and osteogenic differentiation of MSCs may be modulated through a Smad-dependent bone morphogenetic protein (BMP) signaling pathway.

KEYWORDS: mesenchymal stem cells · carbon nanotubes · adipogenic differentiation · osteogenic differentiation · Smad-dependent BMP signaling pathway

RESULTS

Preparation and Characterization of Carboxylated Carbon Nanotubes. SWCNTs (diameter < 2 nm) and MWCNTs (diameter < 5 nm) with the same mean length of 5−15 μm were obtained from Nanotech Port
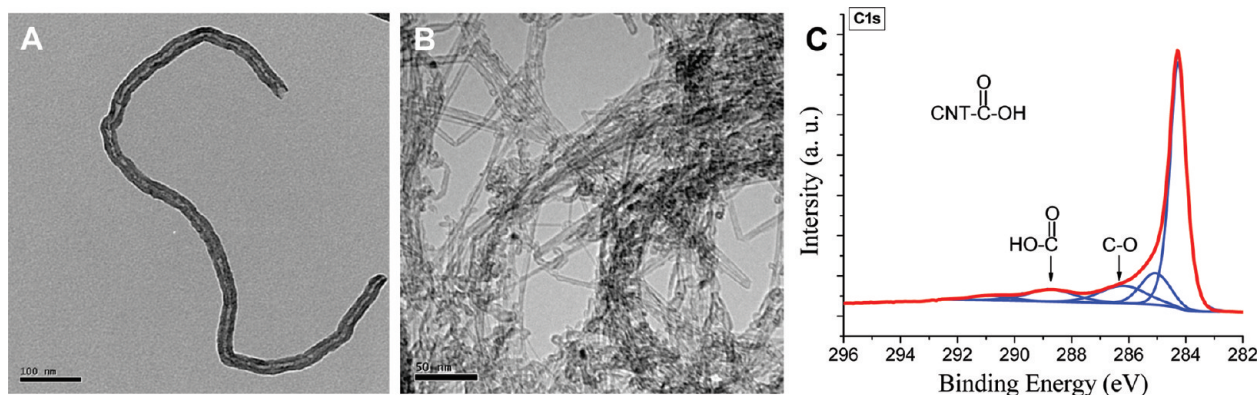
Figure 1. TEM images of carboxylated MWCNTs (A) and carboxylated SWCNTs (B), and XPS spectra (C) of CNTs with carboxylic groups.

(Shenzhen, China). Carboxylated CNTs were generated by refluxing in a mixture of concentrated sulfuric and nitric acids.[11−13] Carboxylated CNTs were washed several times with distilled water by ultracentrifugation (10 000g × 30 min) until the pH reached 7.0, which could not affect the pH of the buffered cellular medium. The CNT suspensions used in the experiments (3, 6, and 30 μg mL^{-1}) were prepared by suspending CNTs with minimum essential medium alpha (α-MEM) supplemented with 10% fetal bovine serum (Gibco Invitrogen, USA). Figure 1A,B shows the transmission electron microscope (TEM) images of SWCNTs and MWCNTs, respectively (obtained with a Phillips Tecnai 12 instrument). X-ray photoelectron spectroscopy (XPS) measurements confirmed the presence of carboxylic groups on CNTs, where the peaks at 288.6 and 286.3 eV of C 1s spectra were ascribed to C═O and C−O (Figure 1C), respectively.

Effects of CNTs on the Viability and Proliferation of MSCs. MTT assay was employed to measure the metabolic activity of the mitochondria of cells based on the principle that liv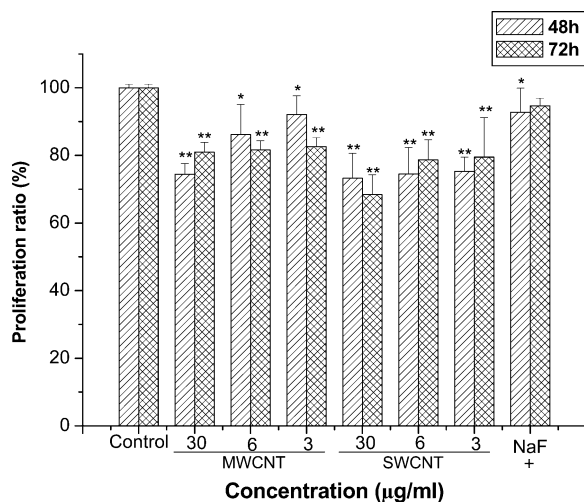ing cells are capable of reducing light color tetrazolium salts into an intense color formazan derivative.[14] Figure 2 shows the viability of MSCs upon treatment with SWCNTs and MWCNTs. The results revealed that CNTs exhibited cytotoxicity on MSCs, where the treatment of MSCs with a series of dilutions (3, 6, and 30 μg mL^{-1}) of CNTs resulted in a decrease in cell viability with the maximum inhibition effect observed after 72 h CNT treatment at the concentration of 30 μg mL^{-1}. Even at the lowest dosage (3 μg mL^{-1}), SWCNTs and MWCNTs decreased the cell viability by 21% and 17% in 72 h, respectively.

Effects of CNTs on the Osteogenic Differentiation of MSCs. Differentiation of pluripotent progenitor MSCs into osteoblasts is a crucial step of osteogenesis. ALP is an ectoenzyme which acts as a marker for cells undergoing differentiation to form preosteoblasts and osteoblasts.[15] Generally, ALP activities were expressed after *in vitro* osteogenic induction for 7 days, while later ALP staining was seen after 14 days of osteogenic induction.[16] Potential effects of CNTs on osteogenic differentiation of MSCs cultured for 7 and 14 days were thus assessed by measuring the ALP activity normalized to total protein content. Figure 3 shows the ALP activity in MSCs cultured with different concentrations of CNTs, with NaF treatment as a positive control.[15] Inhibition of osteogenic differentiation of MSCs was observed for all doses of CNTs on day 7. ALP activity of MSCs was significantly decreased on day 14, as well. CNTs inhibited the ALP activity of MSCs in a time-dependent manner without evident dose dependence.

Effects of CNTs on the Formation of Mineralized Matrix Nodules. An essential sign for the osteogenic differentiation of MSCs is bone matrix maturation and mineralization. After cultured for 2−3 weeks, osteoblast nodes formed and reached peak quantity when osteoblasts started to mineralize.[17] MSCs from bone marrow exhibited mineralization upon treatment with CNTs for 18 and 21 days. The mineralized nodules were counted by staining the fixed cultures with Alizarin Red S (ARS), and the amount of mineralization was quantitated by elution of ARS from stained mineral deposits (Figures 4). MSCs treated with osteogenic supplement (OS) were
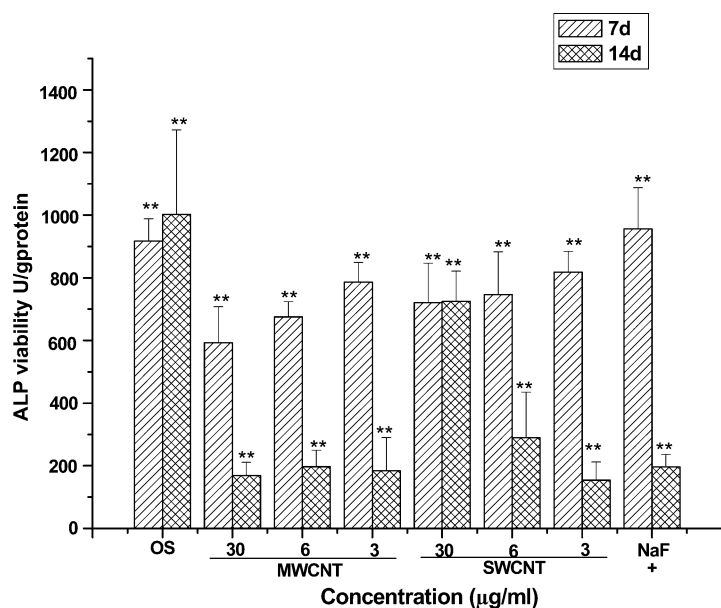

Figure 2. Cytotoxicity in MSCs exposed to carboxylated SWCNTs and carboxylated MWCNTs for 48 and 72 h. Results are mean ± SD of the triplicate experiments, *p < 0.05, **p < 0.01. The cytotoxicity was determined by MTT reduction method.

Figure 3. Effects of carboxylated CNTs on the ALP activity of MSCs. Results are mean ± SD of the triplicate experiments, **$p < 0.01$; 1.0 μM NaF was used as a positive control.

used as normal control, and 1.0 μM NaF was used as the positive control, which promoted mineralization of MSCs by 30% and 50% on day 18 and day 21, respectively. Coupling the number count with quantitation of ARS deposition revealed a dose-dependent decrease in the formation of mineralized nodules upon CNT treatment. Greater than 70% and 50% decreases in the formation of mineralized nodules upon CNT treatment were observed at the dosage of 30 μg mL^{-1} SWCNTs and MWCNTs, respectively. SWCNTs appeared to exhibit slightly greater inhibitory effects at all concentrations (3, 6, and 30 μg mL^{-1}) than MWCNTs.

Effects of CNTs on the Adipocytic Differentiation of MSCs. Adipocytes and osteoblasts all originate from MSCs and have an inversely proportional relationship.[18] Therefore, it is also important to investigate the effects of CNTs on the adipocytic differentiation of MSCs. The adipocytic differentiation rates of MSCs in the absence and presence of CNTs were herein determined by specifically staining intracytoplasmic lipids with Oil Red O.[19] Figure 5A−D shows adipocytic differentiation of MSCs in the absence and presence of CNTs stained by Oil Red O. The results indicated that CNTs also strongly inhibited the adipocytic differentiation of MSCs, where up to 77% and 66% inhibition was observed on day 14 at the dos-
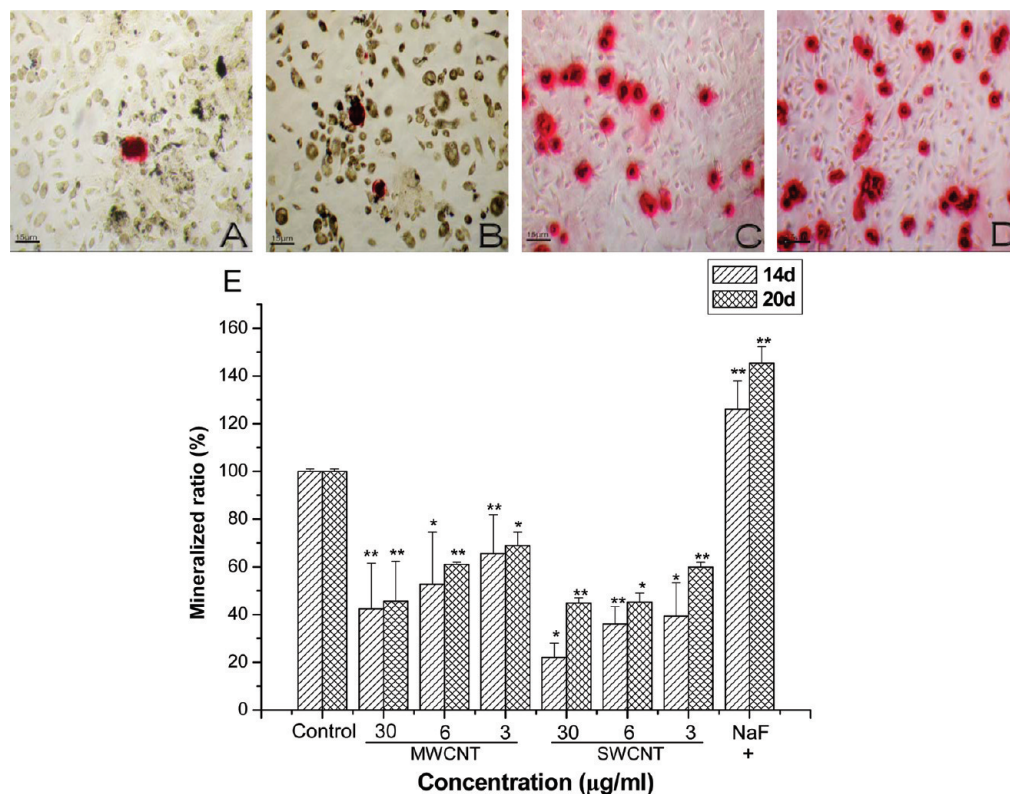

Figure 4. Mineralized nodule formation stained by Alizarin Red S. (A) Cells treated with 30 μg mL^{-1} carboxylated SWCNTs + osteogenic supplement (OS). (B) Cells treated with 30 μg mL^{-1} carboxylated MWCNTs + OS. (C) Cells treated with OS only. (D) Cells treated with 1.0 μM NaF + OS. Original magnification = 100×. (E) Effects of CNTs on the mineralized nodule formation of MSCs. Mineralization quantitated by elution of Alizarin Red S from stained mineral deposits. Results are mean ± SD of the triplicate experiments, **$p < 0.05$, ****$p < 0.01$.
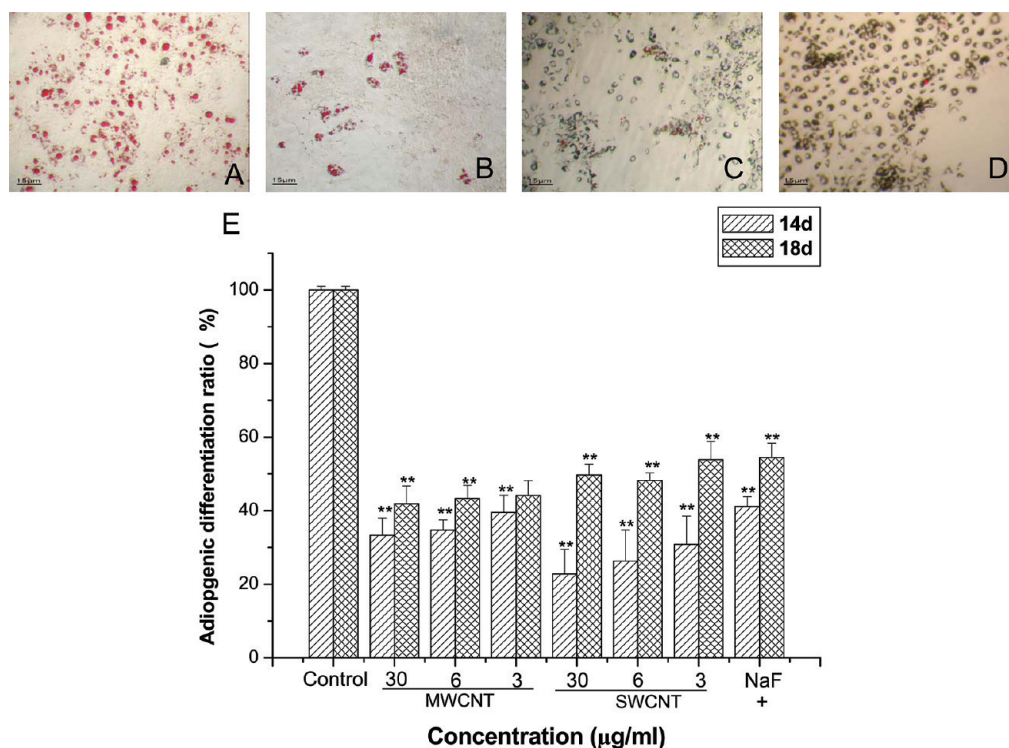
Figure 5. Adipogenic differentiation of MSCs stained by Oil Red O. (A) Cells with adipogenic supplement (AS). (B) Cells treated with AS + 1.0 μM NaF. (C) Cells treated with AS +30 μg mL^{-1} carboxylated SWCNTs. (D) Cells treated with AS + 30 μg mL^{-1} carboxylated MWCNTs. Original magnification = 100$\times$. (E) Dose dependence of CNTs on the adipogenic differentiation of MSCs. Results are mean $\pm$ SD of the triplicate experiments, **$p < 0.01$; 1.0 μM NaF was used as a positive control.

age of 30 μg mL^{-1} of SWCNTs and MWCNTs, respectively. In addition, compared with day 14, the inhibition on adipogenic differentiation was less prominent on day 18.

Scanning Electron Microscopy (SEM) and Transmission Electron Microscopy (TEM). The morphology change of MSCs during the differentiation was investigated using SEM. Figure 6 shows SEM images of MSCs after 7 days of culture in the absence and presence of CNTs. MSCs adhered to substrates by means of thin cytoplasmic digitations or filopodia, and cytoplasmic extensions were flattened and expanded over the entire surface. After 7 days of culture in basal medium without the addition of OS and CNTs, the cells displayed a spindly, fibroblast-like morphology and have formed clusters, which is normal phenotypic behavior of MSCs (Figure 6A−C). As the cells differentiated into osteoblasts in the presence of OS without the treatment of CNTs, they started depositing matrix on the surface. SEM images showed that the whole surface was covered with a network of well spread cells, which acquired a more polygonal morphology (Figure 6D−F). High-magnification SEM images showed the long pseudopodia and cells had multilayered various sizes and shapes (Figure 6F). When treated with CNTs, most of the cells still displayed a spindly, fibroblast-like morphology for both MWCNTs (Figure 6G−I) and SWCNTs (Figure 6J−L), suggesting that the cells did not successfully differentiate to osteoblasts in the presence of CNTs. These results correlated

well with the results of the previous cell assays, where osteogenic differentiation and mineralization of MSCs were inhibited by both SWCNTs and MWCNTs.

Cellular signaling pathways may be affected when CNTs interact with cell surface receptors or with intracellular proteins. The evaluation of cell uptake and intracellular localization of CNTs is crucial for mechanistic understanding of their biological impact.[10] The TEM images clearly showed that, although most of the CNTs did remain in the extracellular space, there were some CNTs taken up by MSCs and grouped in intracellular compartments of cells (Figure 7A−F). Our finding correlates well with the confocal microscopy results that fluorescently labeled derivatized CNTs localized primarily within the cytoplasm[20−22] and the perinuclear region of the cell.[23]

Q-PCR Analysis of Osteogenic and Adipocytic Differentiation Specific Genes. Q-PCR analysis was used to measure the expression of mRNA transcripts of tissue specific molecules in order to reveal the involvement of specific signaling pathways in CNT-modulated inhibition of MSC differentiation. The GAPDH gene was used as the calibrator gene (control), and the relative expression levels of specific genes, including Id1, Id2, Id3, Runx2, BMP-2, Col I, ALP, OCN, PPARγ2, C/EBPα, C/EBPβ, and C/EBPδ, were determined by Q-PCR. The results are presented as an increase or decrease (fold change) in the values of cellular expression of various genes compared to the control. The results showed that several genes that
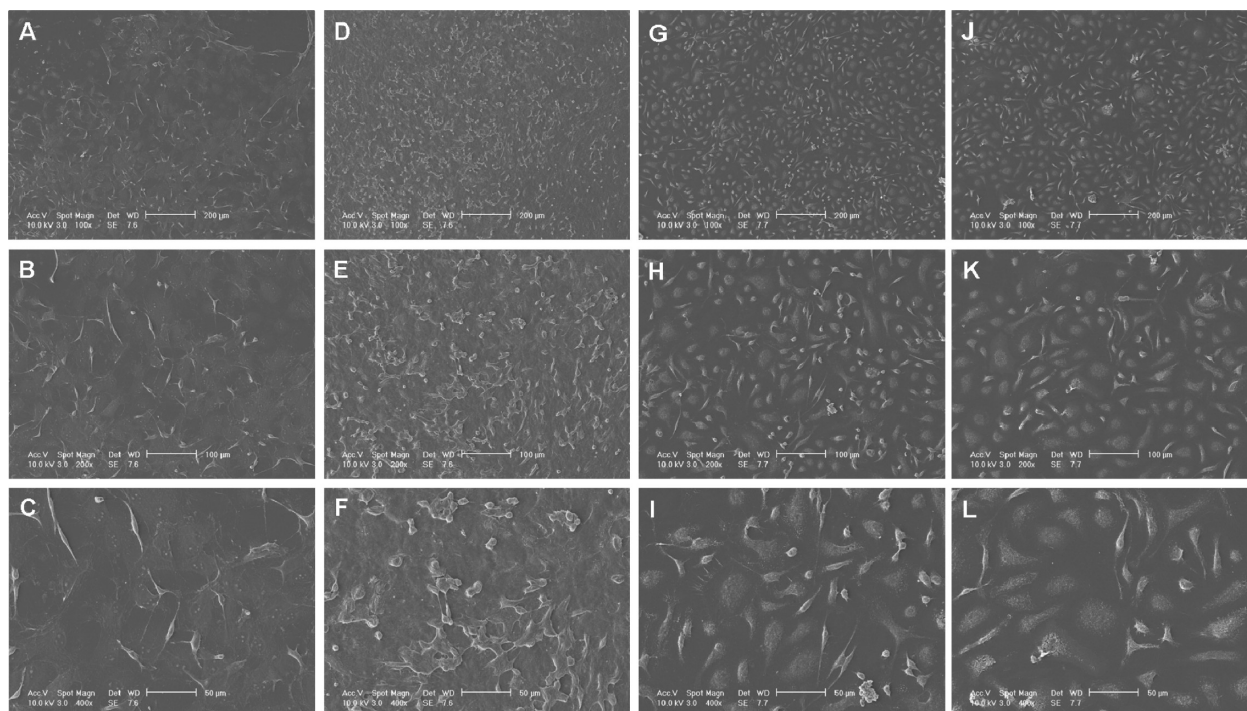
Figure 6. SEM images of MSCs after 7 day culture. (A−C) MSCs were cultured in the absence of CNTs and OS. (D−F) MSCs were treated with OS only. (G−I) MSCs were treated with OS and 30 µg mL^{-1} carboxylated MWCNTs. (J−L) MSCs were treated with OS and 30 µg mL^{-1} carboxylated SWCNTs.

were supposed to be activated during osteogenic differentiation and adipocytic differentiation were significantly down-regulated in the MSCs treated with CNTs as compared to untreated MSCs (Figure 8A,B).

Western Blot Analysis of Key Proteins Involved in the BMP Signaling Pathway. Western blot can be used to detect the expression of a specific protein in a given sample. To demonstrate the suppression of the BMP signaling
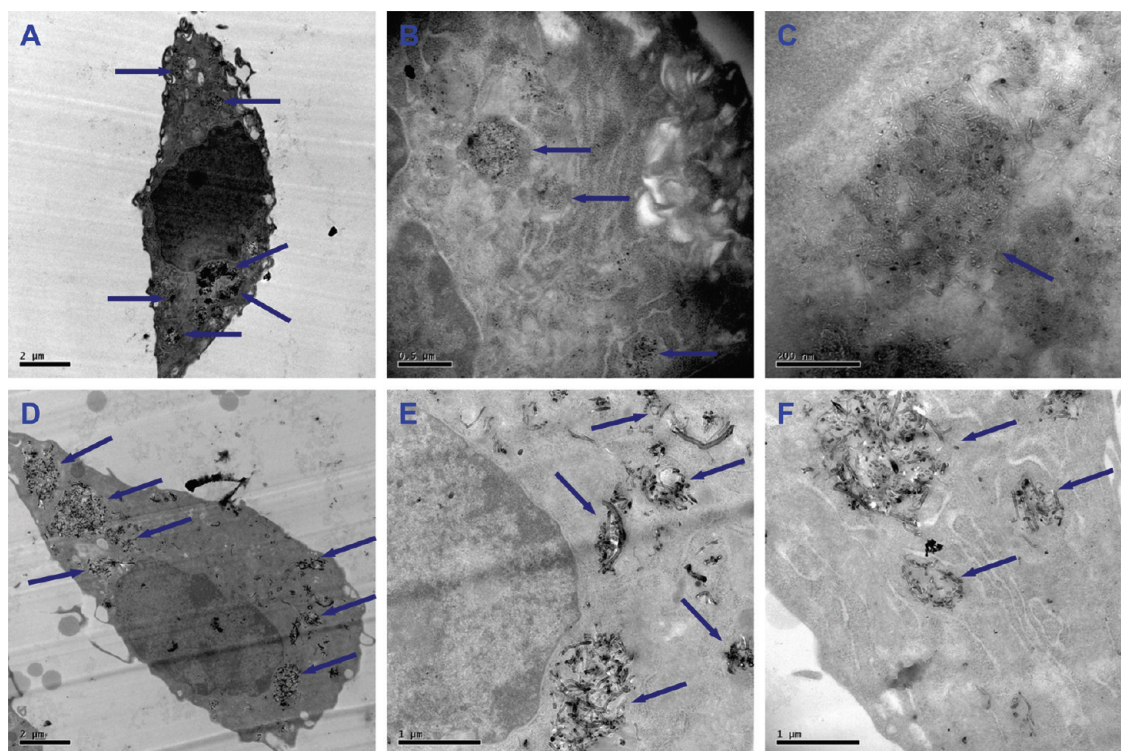

Figure 7. TEM characterization of cell uptake of carboxylated SWCNTs (A−C) and carboxylated MWCNTs (D−F) and their cellular locations in MSCs. MSCs were incubated with carboxylated CNTs (30 µg mL^{-1}) for 7 days. Arrows indicate the CNTs.
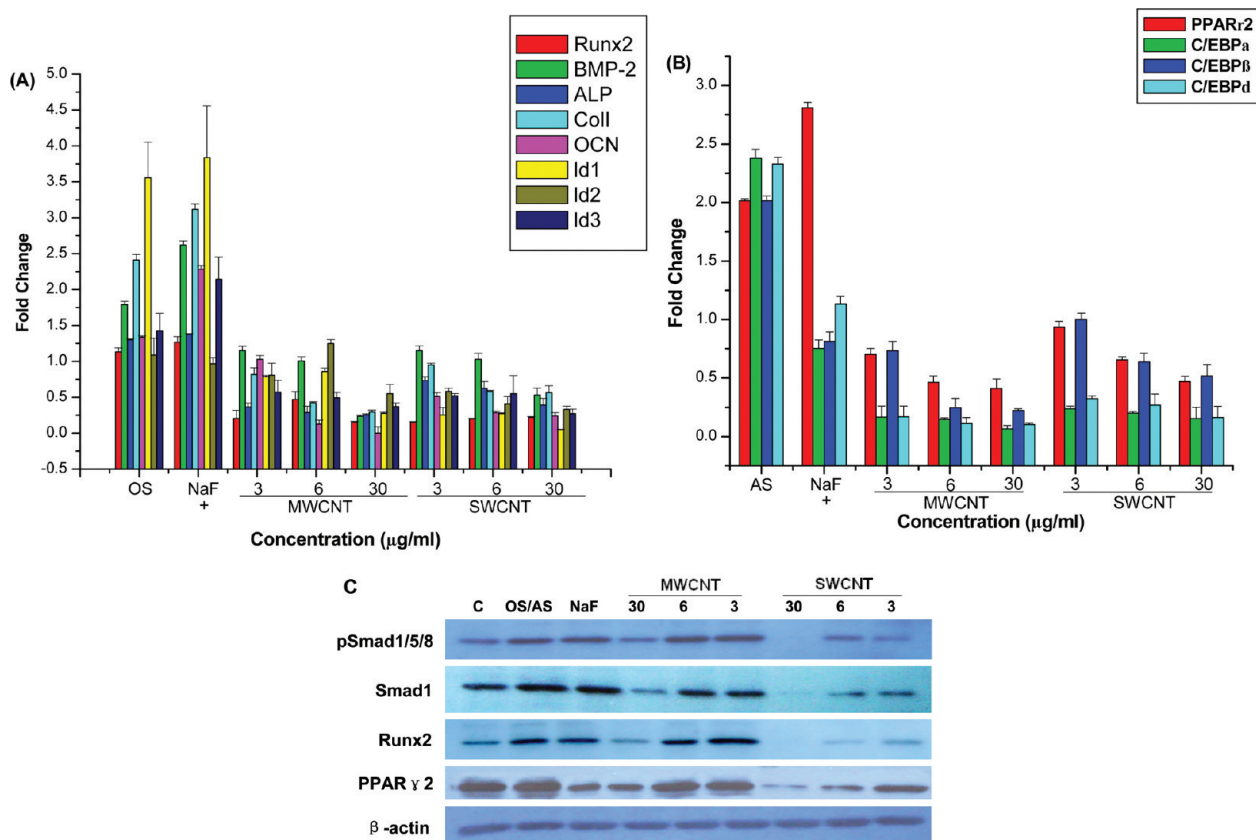
Figure 8. Q-PCR analysis for the expression of osteogenic differentiation specific genes (A) and adipocytic differentiation specific genes (B) under the induced conditions. Results are mean ± SD of the triplicate experiments, *$p < 0.05$. (C) Western blot analysis for Smad1, pSmad1/5/8, Runx2, and PPARγ proteins in MSCs treated with carboxylated CNTs after 7 day incubation. β-Actin protein expression was used as a loading control. Proteins from each lysate were separated in SDS-PAGE.

pathway and subsequent inhibition of MSC differentiation, the expression levels of key proteins involved in the BMP signaling pathway, such as Smad protein and phosphorylated Smad proteins (pSmad1/5/8), and the master transcription factors proteins, such as Runx2 and PPARγ proteins, were measured. Western blotting results showed that the expression of Smad1, pSmad1/5/8, Runx2, and PPARγ proteins was significantly reduced in MSCs treated with CNTs (Figure 8C).

Detection of ROS Production and the Metal Impurities Trapped Inside the CNTs. One possible mechanism of CNT-induced cytotoxicity is that ROS generated by CNTs could suppress proliferation and differentiation of MSCs.[25] Intracellular levels of ROS were thus measured with the fluorescent dye 2′,7′-dichlorofluorescein diacetate (DCFH-DA). DCFH-DA is diffused into cells and deacetylated by cellular esterases to nonfluorescent 2′,7′-dichlorodihydrofluorescein (DCFH), which is rapidly oxidized to highly fluorescent 2′,7′-dichlorodihydrofluorescein (DCF) by ROS.[24] As shown in Table 1, no fluorescent signals from DCF can be detected in MSCs cultured in the presence of CNTs, suggesting that no ROS were generated by carboxylated CNTs. Inductively coupled plasma mass spectroscopy (ICP-MS) experiments revealed that 34.8 ppm of Fe and 70.7 ppm of Co existed in the pristine CNTs. After strong acid treatment to produce carboxylated CNTs, the concentrations of Fe and Co were decreased to 5.6 and 9.4 ppb, respectively. The ICP-MS results indicated that no ROS were able to be generated by the carboxylated CNTs used in this study.

DISCUSSIONS

Nanomaterials interacting with cells establish a series of nanomaterial−biological interfaces that could lead to intracellular uptake and have biocompatible or bioadverse outcomes.[25] TEM images clearly showed

TABLE 1. ROS in MSCs Treated with CNTs[a]

	control	positive control	MWCNTs (μg mL^{-1})			SWCNTs (μg mL^{-1})		
			3	6	30	3	6	30
48 h	1.71 ± 0.06	3.87 ± 0.06[b]	1.71 ± 0.12	1.71 ± 0.12	1.72 ± 0.09	1.71 ± 0.04	1.71 ± 0.07	1.73 ± 0.02
72 h	1.57 ± 0.08	3.88 ± 0.16[b]	1.58 ± 0.12	1.58 ± 0.12	1.59 ± 0.31	1.58 ± 0.13	1.58 ± 0.06	1.59 ± 0.21

[a]Data are mean ± SD of the triplicate experiments. [b]**$p < 0.01$. Unit for fluorescence intensity is arbitrary unit.

that CNTs were internalized and localized primarily within the cytoplasm and the perinuclear region of MSCs (Figure 7A−F). MTT results revealed a significant cytotoxicity of CNTs on MSCs (Figure 2). SEM characterization also provided substantial evidence that cell number decreased after the treatment with CNTs and most of the MSCs did not successfully differentiate to osteoblasts in the presence of CNTs (Figure 6). Toxicological activity of CNTs depends on the interactions with the cell surface and mechanisms of transmission into the cytosol and nucleus.[26] The main characteristics of CNTs, such as small size and large surface area, may be responsible for the material interactions that could result in their toxicological effects. The properties of CNTs also resulted in a catalytic activity which may contribute to a new aggressive form of long-term toxicity.[27] The nanomaterial size is an important factor in their cytotoxicity assessment, where the cytotoxicity of CNTs on macrophages is apparently based on SWCNTs > MWCNTs > C_{60}[28] and/or graphite > SWCNTs > C_{60}.[29] We have also reported that CNTs reduced the viability of primary osteoblasts in time- and dose-dependent manners in the order of SWCNTs > DWCNTs > MWCNTs.[30] Although in this study we did not observed a definite correlation between the inhibition of MSC and the size of CNTs in several cellular assays, SWCNTs seem to exhibit stronger effects than MWCNTs.

There are also reports suggesting low cytotoxicity or no signs of cytotoxicity of CNTs.[20−22,31−39] Especially, if CNTs are bound to a surface, no toxicity has been reported at all.[7,33−35] CNT-based substrates have been demonstrated to support dendrite elongation and cell adhesion[7] and improve neural signal transfer,[33] as well as support other cell types such as fibroblasts[34] and osteoblasts.[35] The surface chemistry also plays a vital role in determining the cytotoxic potential of CNTs.[27] Thus, surface functionalization of CNTs with specific chemical[8,9,20,21] and/or biological species[22,36,37] may be a feasible route to develop biocompatible CNTs. Recently, CNT scaffolds have also been demonstrated to modulate stem cell lineage commitment toward neurogenesis when coupled with soluble chemical factors.[38,39]

Cells maintain their homeostasis through a comprehensive signaling network. Any perturbation of this system by nanomaterials will influence cell function and behavior.[40] The results from ALP activity assay suggested a substantial decrease of ALP activity upon CNT treatment. About 30% and 20% ALP activity decrease was observed at the dosage of 30 μg mL^{-1} SWCNTs and MWCNTs, respectively (Figure 3). CNTs inhibited the ALP activity of MSCs in a time-dependent manner without evident dose dependence, which may be caused by the different differentiation states of the MSCs. It has been recognized that ALP activity rises during the proliferation period and reaches a maximum level as the culture progresses into the mineralization stage. How-

ever, the cellular levels of ALP decline in heavily mineralized cultures.[41] The appearance of ALP activity is an early phenotypic marker for osteogenic differentiation of MSCs, while mineralized nodule formation is a phenotypic marker for the last stage of mature osteoblasts. Coupling the number count with quantitation of ARS deposition revealed a greater than 70% and 50% decrease in the formation of mineralized nodules upon CNT treatment at the dosage of 30 μg mL^{-1} SWCNTs and MWCNTs, respectively (Figure 4). These data strongly suggested that carboxylated CNTs inhibited the proliferation and osteogenic differentiation of MSCs.

Currently, there are two established cytotoxicity mechanisms: oxidative stress and disruption of intracellular metabolic pathways.[25,27] Pristine CNTs have been shown to generate ROS and cause cell apoptosis via tje NF-κB signaling pathway.[42] In order to verify that ROS generated by CNTs could suppress proliferation and differentiation of MSCs, intracellular levels of ROS were measured with the fluorescent dye 2′,7′-dichlorofluorescein diacetate (DCFH-DA). However, the results revealed no detectable fluorescent signals from DCF (Table 1), suggesting that no ROS were generated by carboxylated CNTs. It has been recognized that the metal impurities trapped inside the CNTs may be partially responsible for ROS generation.[25,43] We used ICP-MS to measure the concentration of metal catalysts and showed that concentration of metals decreased from 106 ppm to 15 ppb after strong acid treatment of pristine CNTs to produce carboxylated CNTs, indicating that no ROS were able to be generated by carboxylated CNTs.[25] All of these data strongly suggested that oxidative stress might not be responsible for the observed decreased proliferation and differentiation of MSCs upon their interaction with carboxylated CNTs.

Recent study demonstrated that carboxylated SWCNTs inhibited cell proliferation by suppressing the BMP signaling pathway.[10] It is well-known that the Smad1-dependent BMP signaling pathway plays an important role in osteogenic differentiation of MSCs.[44] Therefore, we hypothesized that the inhibition of proliferation and osteogenic differentiation of MSCs is modulated through a Smad-dependent BMP signaling pathway. Western blotting results demonstrated the suppression of the BMP signaling pathway during the inhibition of osteogenic differentiation by CNTs. The expression levels of key proteins involved in the BMP signaling pathway, such as Smad protein and phosphorylated Smad proteins (pSmad1/5/8), and the osteogenic master transcription factors, such as Runx2 protein, were significantly reduced (Figure 8C). Phosphorylated Smad proteins translocate into the nucleus, bind promoters of target genes, and regulate the transcription. The inhibition of Smad phosphorylation by CNTs may cause a decrease in nucleus translation.[10] The data indi-

cated that the Smad1-dependent BMP signaling was suppressed by carboxylated CNTs, leading to subsequent down-regulation of the expression of osteogenic genes underlying the phenotype of terminally differentiated osteocytes.

Id genes are known to be the direct targets of the BMP signaling pathway, whose transcription is activated by BMP receptor signaling through Smad-dependent pathways.[45] The lineage commitment gene Runx2 belongs to the Runx family and plays a vital role in determining the osteoblast lineage from the pluripotent MSCs. It has been demonstrated that in the absence of Runx2 no osteoblast differentiation can be observed.[46] BMPs are responsible for enhancing osteoblastic differentiation, including stimulation of the expression of bone structural proteins such as Col-I and OCN, and the mineralization of bone matrix.[47] During the proliferation period, the genes associated with the formation of ECM components (such as type-I collagen and fibronectin) are activated. Type-I collagen is the most abundant protein found in the organic bone matrix and plays an essential role in influencing cellular behavior.[48] ALP is responsible for removing phosphate groups from many types of molecules, including nucleotides, proteins, and alkaloids. ALP is considered to be important in producing bone mineral and is a marker for cells that are undergoing differentiation forming preosteoblasts and osteoblasts.[15] Osteocalcin (OCN) is the most specific gene for the osteoblast differentiation and mineralization. OCN is expressed during the postproliferative period and reaches its maximum expression during mineralization and accumulates in the mineralized bone.[16] MSCs cultured in medium conducive for osteogenic differentiation in the presence of CNTs exhibited the down-regulation of all these osteoblast specific genes (Figure 8A), which is consistent with the observed inhibitory effects of CNTs on ALP activity (Figure 3) and mineralized matrix nodule formation of MSCs (Figure 4).

Because of the reciprocal relationship between the differentiation of adipocytic and osteogenic cells in the MSC culture, it is expected that the inhibition of osteogenic differentiation of MSCs may result in the promotion of adipocytic differentiation of MSCs. Howerver, our results showed that CNTs also strongly inhibited the adipocytic differentiation of MSCs, where up to 77% and 66% inhibition was observed at the dosage of 30 μg mL^{-1} of SWCNTs and MWCNTs, respectively. Adipogenesis is a highly regulated process in which a coordinated cascade of transcription factors leads to the formation of mature adipocytes. This cascade begins with the transient expression of CCAAT/enhancer binding protein β (*C/EBP*β) and *C/EBP*δ, which activate *C/EBP*α and peroxisome proliferator-activated receptor γ (*PPAR*γ).[49] *C/EBP*α and *PPAR*γ together coordinate the expression of adipogenic genes underlying the phenotype of terminally differentiated adipocytes.[49] The ex-
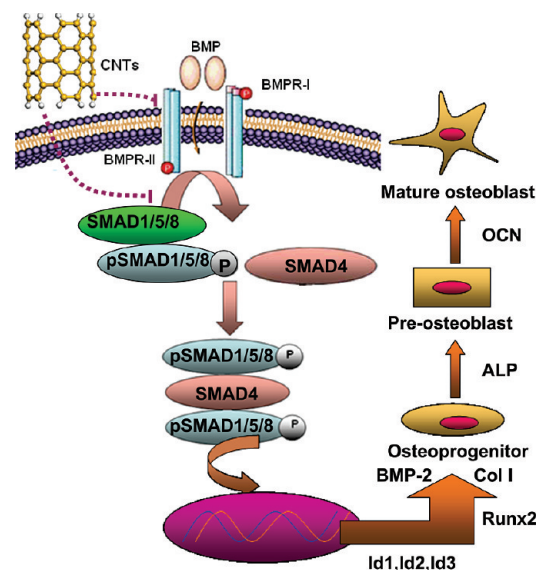

Figure 9. Plausible mechanism of the modulation of proliferation and osteogenic differentiation of MSCs through the Smad-dependent BMP signaling pathway.

pression of adipocytic differentiation specific genes and protein was also down-regulated when MSCs were cultured in the presence of adipogenic supplement and CNTs (Figure 8B,C), which is consistent with the observed dose-dependent inhibitory effects of CNTs on adipogenic differentiation of MSCs (Figure 5).

On the basis of the above findings, a schematic model was proposed to describe the modulation of proliferation and osteogenic differentiation of MSCs through the Smad-dependent BMP signaling pathway (Figure 9). CNTs likely suppress the BMP signaling pathway by interacting with proteins at the cell membrane or in the cytoplasm. The blockage of the BMP signaling pathway leads to down-regulation of the osteogenic master transcription factor, Runx2, which subsequently down-regulates osteoblast marker genes Col I and BMP2 at early stages and ALP and OCN at later stages of differentiation.[44] Although a number of genes involved in adipocytic differentiation were shown to be down-regulated upon CNT treatment, the molecular mechanism involved in the inhibition of adipocytic differentiation of MSCs upon their exposure to CNTs requires further study.

CONCLUSIONS

In conclusion, the results showed that CNTs inhibited the proliferation, osteogenic differentiation, adipogenic differentiation, and mineralization of MSCs during short- and long-term osseointegration *in vitro*. The results from the oxidative stress assay indicated that ROS may not be responsible for the observed cytotoxicity of carboxylated CNTs. The expression of a panel of osteoblast specific genes and adipocyte specific genes was significantly attenuated during the differentiation of MSCs in the presence of CNTs. Q-PCR results and Western blot analysis together confirmed that the inhi-

bition of proliferation and osteogenic differentiation of MSCs is related to the Smad-dependent BMP signaling pathway. The study suggests that the safety profile of CNTs should be more thoroughly investigated in order to provide better understanding for their design and applications as biocompatible nanomaterials.

EXPERIMENTAL METHODS

Isolation and Culture of MSCs. MSCs were prepared from 6 week old specific pathogen free (SPF) Kunming mice (Southern Medical University, China) following the Kelly method.[50] In brief, the mice were executed by cervical vertebra. Femora and tibiae were aseptically harvested, and the whole bone marrow was flushed using supplemented α-MEM in a 10 mL syringe and a 25 gauge needle. Suspended whole bone marrow was washed by α-MEM. The cells were collected and cultured in α-MEM with 10% heat-inactivated fetal bovine serum, 100 U/mL penicillin (BBI, Canada), and 100 μg mL^{-1} streptomycin (BBI, Canada), for 3 days in a humidified atmosphere of 5% CO$_2$ in air at 37 °C, then replaced with fresh medium. The culture medium was changed every 3 days during the experiments.

MSCs Viability and Proliferation Assay. MTT assay was used to determine viability and proliferation of MSCs upon treatment with CNTs, as described in detail elsewhere.[14,30] MSCs were seeded in 96-well tissue culture plates at the density of 4×10^6 cells per well and incubated for 3 days. After the treatment with CNTs for 48 and 72 h, the plates were washed twice with culture medium, and then MTT was added and incubated for another 4 h. Cells without CNT treatment were used as a control. The relative cytotoxicity was expressed as percentage of [OD$_{sample}$ − OD$_{blank}$]/[OD$_{control}$ − OD$_{blank}$] × 100. Each experiment was performed in triplicate.

Alkaline Phosphatase (ALP) Activity Assay for Osteogenic Differentiation of MSCs. Alkaline phosphatase (ALP) is an early marker of the MSCs' osteogenic differentiation. Therefore, an ALP activity assay was used to evaluate the osteogenic differentiation of MSCs, as described in detail elsewhere.[30] MSCs were seeded in 48-well tissue culture plates at the density of 5×10^6 cells per well with the osteogenetic induction supplement. A series of dilutions (3, 6, and 30 μg mL^{-1}) of CNTs were added to the culture medium with osteogenic induced supplement for 7 and 14 days. NaF (Sigma, St Louis, MO), which can promote osteogenetic differentiation of MSCs, was used as a positive control and dispersed in α-MEM. All results were normalized by protein content.

Oil Red O Staining Assay for Adipogenic Differentiation of MSCs. Oil Red O staining assay was used to evaluate adipogenic differentiation of MSCs, as described in detail elsewhere.[19,30] MSCs (1×10^7 cells per well) were seeded in 48-well tissue culture plates and cultured for 14 and 18 days. The adipogenetic induced supplements (10 mg L^{-1} insulin, 1.0×10^{-7} mol L^{-1} dexamethasone) and CNTs of different concentrations (final concentrations of 3, 6, and 30 μg mL^{-1}) were added to the culture medium. Fat droplets within differentiated adipocytes from MSCs were evaluated by the Oil Red O staining method. The adipogenetic differentiation inhibition was expressed as a percentage of [OD$_{sample}$ − OD$_{blank}$]/[OD$_{control}$ − OD$_{blank}$] × 100.

Assay for Mineralized Matrix Formation. Alizarin Red S staining assay was used to evaluate mineralized matrix formation, as described in detail elsewhere.[30,51] MSCs (5×10^6 cells per well) were seeded in 48-well tissue culture plates and cultured for 3 days. The medium was then changed to medium containing osteogenetic induced supplements in the presence of 3, 6, and 30 μg mL^{-1} of CNTs or NaF for 18 and 21 days. The formation of mineralized matrix nodules was determined by ARS staining. The mineralization inhibition rate was expressed as a percentage of [OD$_{sample}$ − OD$_{blank}$]/[OD$_{control}$ − OD$_{blank}$] × 100.

Scanning Electron Microscopy (SEM) and Transmission Electron Microscopy (TEM). Cell morphology with and without the treatment of CNTs was observed by SEM after 7 days of culture, as described in detail elsewhere.[52,53] In brief, MSCs were harvested and rinsed twice in PBS and subsequently soaked in the primary fixative of 2% glutaraldehyde for 1 h and postfixed for 1 h at 4 °C with 1% osmium tetroxide before dehydration with increasing concentrations of ethanol and finally with hexamethyldisila-

zane (HMDS) to further extract water. The dehydrated MSCs were maintained in desiccators for overnight air drying. After sputter-coating with carbon, SEM imaging was conducted on FEI Nova SEM system at an accelerating voltage of 10 kV. For TEM imaging, MSCs were prefixed in modified Karnovsky fixative (2% glutaraldehyde + 2% paraformaldehyde) in 0.1 M cacodylate buffer (pH 7.4) with 0.05% CaCl$_2$ solution at 4 °C for 2 h after a 7 day incubation in the presence of 30 μg mL^{-1} CNTs. The cells were then postfixed in 1% osmium tetroxide and subsequently dehydrated in a graded series of ethanol and acetone solution and embedded in resin. Semi-thin sections were cut perpendicularly to the cells layers with a diamond knife, mounted on glass slides, stained with methylene blue, and then examined under light microscopy for orientation purposes. Ultrathin sections were performed, collected on copper grids, and stained with 5% uranyl acetate in water for 4 min and lead citrate for 2 min. The ultrastructural alterations and internalization of CNTs were observed with a Phillips Tecnai 12 instrument operating at 80 kV. All SEM and TEM microscopic related reagents were obtained from Electron Microscopy Sciences, USA.

Quantitative Real-Time Polymerase Chain Reaction (Q-PCR). Total RNA from MSCs, which were treated by CNTs for 7 days, was extracted using Trizol Plus RNA purification kit (Invitrogen) and were reverse transcribed to first-strand cDNA according to the TaKaRa protocol (TaKaRa, Tokyo). Q-PCR was performed in a total volume of 25 μL with 1 μL of cDNA, 1 μL gene specific 10 μM PCR primer pair stock, and 12.5 μL RT^2 SYBR Green/ROX Q-PCR Master Mix (SABiosciences, USA) using ABI 7000 Sequence Detection System (Applied Biosystems, USA). The PCR profile began with 10 min at 95 °C to activate Hotstart TaqDNA polymerase and then followed by 40 cycles of 15 s at 95 °C and 1 min at 60 °C, and later followed by the melting curve test. The relative amount of mRNA expression normalized to GAPDH was expressed as fold change, which was calculated by the comparative C_T ($2^{-\Delta\Delta C_T}$) relative to the control group as a reference: $2^{-\Delta\Delta C_T} = 1$. The primer sequences are listed in Table 2.

Western Immunoblotting. MSCs were washed with cold PBS and lysed in cold 50 mM Tris-HCl (pH 7.4), 10 mM EDTA, 4.3 M urea, and 1% Triton X-100 (USB Corporation, Japan). Proteins were subjected to SDS-PAGE using 10% gel for detection of Smad1, pSmad1/5/8, Runx2, and PPARγ and transferred onto a nitrocellulose membrane (Amersham Biosciences, UK). The membrane was blocked overnight at 4 °C with 5% bovine serum albumin (Sigma, St Louis, MO) in TBST solution (10 mM Tris HCl pH 8.0, 150

TABLE 2. Primer Pair Sequences for the Q-PCR Study

gene[a]	forward primer sequence (5′—3′)	reverse primer sequence (5′—3′)
ALP	GTTGCCAAGCTGGGAAGAACAC	CCCACCCCGCTATTCCAAAC
BMP-2	TGGCCCATTTAGAGGAGAACC	AGGCATGATAGCCCGGAGG
Col I	AACATGACCAAAAACCAAAAGTG	CATTGTTTCCTGTGTCTTCTGG
ERα-1	GAATCCACATGCCTATTGC	AGAACCCACTGACCCATT
OCN	GAACAGACTCCGGCGCTA	AGGGAGGATCAAGTCCCG
Runx2	TTCTCCAACCCACGAATGCAC	CAGGTACGTGTGGTAGTGAGT
GAPDH	GACTTCAACAGCAACTCCCAC	TCCACCACCCTGTTGCTGTA
PPARγ2	TGTGGGGATAAAGCATCAGGC	CCGGCAGTTAAGATCACACCTAT
C/EBPα	GTGCTTCATGGAGCAAGCCAA	TGTCGATGGAGTGCTCGTTCT
C/EBPβ	GCGCGAGCGCAACAACATCG	CAGCACAGGCTGTTGACCATCATA
C/EBPδ	GAGCGTCCTACGCGCCAGTAC	GATCACGGAGCTGTGCCGGTC

[a]ALP, alkaline phosphatase; BMP-2, bone morphogenetic protein 2; Col I, collagen type-I; ERα-1, estrogen receptor α 1; OCN, osteocalcin; Runx2, runt related transcription factor 2; PPARγ2, peroxisome proliferator activated receptor γ 2; C/EBPα, CCAAT enhancer binding protein α; C/EBPβ, CCAAT enhancer binding protein β; C/EBPδ, CCAAT enhancer binding protein δ.

mM NaCl, 0.05% Tween-20). Then, the blots were incubated with anti-Smad1, anti-pSmad1/5/8, anti-Runx2, anti-PPARγ, or anti-β-actin primary antibodies (Santa Cruz Biotechnology, Inc.) in the TBST solution at a 1:1000 dilution for 2 h at room temperature, followed by 1 h incubation with antirabbit, antigoat antibodies conjugated with horseradish peroxidase, and visualized with an enhanced chemiluminescence (ECL) kit (Amersham Biosciences, UK).

Detection of ROS production and the metal impurities trapped inside the CNTs. Intracellular levels of ROS were assessed using reactive oxygen species assay kit (Beyotime, China) which detects hydrogen peroxide, peroxyl radicals, and peroxynitrite anions. The assay employs the cell-permeable fluorogenic probe 2′,7′-dichlorodihydrofluorescein diacetate (DCFH-DA). In brief, MSCs were seeded in 96-well tissue culture plates at the density of 4×10^6 cells per well and incubated for 3 days. After the addition of CNT suspensions, 48 and 72 h further incubation was performed. Cells incubated with ROSUP (5.0 mg mL^{-1}) for 20 min were used as a positive control, and cells without CNT treatment were used as a negative control. Then, cells were incubated with 10 μM DCFH-DA in the dark for 30 min. Data were collected using a fluorescence microplate reader. DCFH excitation and emission wavelengths were at 488 and 525 nm, respectively. ICP-MS was employed to determine the metal impurities trapped inside the CNTs. In brief, 0.21 g of pristine CNTs or carboxylated CNTs was dissolved in 10 mL of concentrated HNO$_3$ and filtered using a 0.22 μm filter. The solution was diluted 25 times for ICP-MS detection. Concentrated HNO$_3$ was set as a blank.

Statistical Analysis. Data were collected from three separate experiments and expressed as means ± standard deviation (SD). The statistical differences were analyzed by a paired student's t-test. P values less than 0.05 were considered to indicate statistical differences.

REFERENCES AND NOTES

1. Pittenger, M. F.; Mackay, A. M.; Beck, S. C.; Jaiswal, R. K.; Douglas, R.; Mosca, J. D.; Moorman, M. A.; Simonetti, D. W.; Craig, S.; Marshak, D. R. Multilineage potential of adult human mesenchymal stem cells. *Science* **1999**, *284*, 143–147.

2. Jiang, Y.; Jahagirdar, B. N.; Reinhardt, R. L.; Schwartz, R. E.; Keene, C. D.; Ortiz-Gonzalez, X. R.; Reyes, M.; Lenvik, T.; Lund, T.; Blackstad, M.; Du, J. B.; Aldrich, S.; Lisberg, A.; Low, W. C.; Largaespada, D. A.; Verfaillie, C. M. Pluripotency of mesenchymal stem cells derived from adult marrow. *Nature* **2002**, *413*, 41–49.

3. Oreffo, R. O. C.; Cooper, C.; Mason, C.; Clements, M. Mesenchymal stem cells: lineage, plasticity and skeletal therapeutic potential. *Stem. Cell. Rev.* **2005**, *1*, 169–178.

4. Chen, R. J.; Zhang, Y. G.; Wang, D. W.; Dai, H. J. Noncovalent sidewall functionalization of single-walled carbon nanotubes for protein immobilization. *J. Am. Chem. Soc.* **2001**, *123*, 3838–3839.

5. Haick, M.; Hakim, M.; Patrascu, M.; Levenberg, C.; Shehada, N.; Nakhoul, F.; Abassi, Z. Sniffing chronic renal failure in rat model by an array of random networks of single-walled carbon nanotubes. *ACS Nano* **2009**, *3*, 1258–1266.

6. Heller, D. A.; Baik, S.; Eurell, T. E.; Strano, M. S. Single-walled carbon nanotube spectroscopy in live cells: towards long-term labels and optical sensors. *Adv. Mater.* **2005**, *17*, 2793–2799.

7. Hu, H.; Ni, Y. C.; Montana, V.; Haddon, R. C.; Parpura, V. Chemically functionalized carbon nanotubes as substrates for neuronal growth. *Nano Lett.* **2004**, *4*, 507–511.

8. Narita, N.; Kobayashi, Y.; Nakamura, H.; Maeda, K.; Ishihara, A.; Mizoguchi, T.; Usui, Y.; Aoki, K.; Simizu, M.; Kato, H.; Ozawa, H.; Udagawa, N.; Endo, M.; Takahashi, N.; Saito, N. Multiwalled carbon nanotubes specifically inhibit osteoclast differentiation and function. *Nano Lett.* **2009**, *9*, 1406–1413.

9. Mooney, E.; Dockery, P.; Greiser, U.; Murphy, M.; Barron, V. Carbon nanotubes and mesenchymal stem cells: biocompatibility, proliferation and differentiation. *Nano Lett.* **2008**, *8*, 2137–2143.

10. Mu, Q. X.; Du, G. Q.; Chen, T. S.; Zhang, B.; Yan, B. Suppression of human bone morphogenetic protein signaling by carboxylated single-walled carbon nanotubes. *ACS Nano* **2009**, *3*, 1139–1144.

11. Chen, W. W.; Tzang, C. H.; Tang, J. X.; Yang, M. S.; Lee, S. T. Covalently linked deoxyribonucleic acid with multiwall carbon nanotubes: synthesis and characterization. *Appl. Phys. Lett.* **2005**, *86*, 103114–103117.

12. Yi, C. Q.; Fong, C. C.; Chen, W. W.; Qi, S. J.; Tzang, C. H.; Lee, S. T.; Yang, M. S. Interactions between carbon nanotubes and DNA polymerase and restriction endonucleases. *Nanotechnology* **2007**, *18*, 025102.

13. Yi, C. Q.; Zhang, Q.; Fong, C. C.; Lee, S. T.; Yang, M. S. The structure and function of ribonuclease A upon interacting with carbon nanotubes. *Nanotechnology* **2008**, *19*, 095102.

14. Carmichael, J.; Degraff, W. G.; Gazdar, A. F.; Minna, J. D.; Mitchell, J. B. Evaluation of a tetrazolium-based semiautomated colorimetric assay—assessment of chemosensitivity testing. *Cancer. Res.* **1987**, *47*, 936–942.

15. Farley, J. R.; Wergedal, J. E.; Baylink, D. J. Fluoride directly stimulates proliferation and alkaline phosphatase activity of bone-forming cells. *Science* **1983**, *4621*, 330–332.

16. Abdallah, B. M.; Jensen, C. H.; Gutierrez, G.; Leslie, R. G. Q.; Jensen, T. G.; Kassem, M. Regulation of human skeletal stem cells differentiation by Dlk1/Pref-1. *J. Bone Miner. Res.* **2004**, *19*, 841–852.

17. Stein, G. S.; Lian, J. B. Molecular mechanisms mediating proliferation/differentiation interrelationships during progressive development of the osteoblast phenotype. *Endocr. Rev.* **1993**, *14*, 424–442.

18. Beresford, J. N.; Bennett, J. H.; Devlin, C.; Leboy, P. S.; Owen, M. E. Evidence for an inverse relationship between the differentiation of adipocytic and osteogenic cells in rat marrow stromal cell cultures. *J. Cell. Sci.* **1992**, *102*, 341–351.

19. Sekiya, I.; Larson, B. L.; Smith, J. R.; Pochampally, R.; Cui, J. G.; Prockop, D. J. Expansion of human adult stem cells from bone marrow stroma: conditions that maximize the yields of early progenitors and evaluate their quality. *Stem Cells* **2002**, *20*, 530–541.

20. Isobe, H.; Tanaka, T.; Maeda, R.; Noiri, E.; Solin, N.; Yudasaka, M.; Iijima, S.; Nakamura, E. Preparation, purification, characterization and cytotoxicity assessment of water-soluble, transition-metal free carbon nanotube aggregates. *Angew. Chem., Int. Ed.* **2006**, *45*, 6676–6680.

21. Dumortier, H.; Lacotte, S.; Pastorin, G.; Marega, R.; Wu, W.; Bonifazi, D.; Briand, J. P.; Prato, M.; Muller, S.; Bianco, A. Functionalized carbon nanotubes are non-cytotoxic and preserve the functionality of primary immune cells. *Nano Lett.* **2006**, *7*, 1522–1528.

22. Pantarotto, D.; Singh, R.; McCarthy, D.; Efhardt, M.; Briand, J. P.; Prato, M.; Kostarelos, K.; Bianco, A. Functionalized carbon nanotubes for plasmid DNA gene delivery. *Angew. Chem., Int. Ed.* **2004**, *43*, 5242–5246.

23. Kostarelos, K.; Lacerda, L.; Pastorin, G.; Wu, W.; Wieckowsk, S.; Luangsivilay, J.; Godefroy, S.; Pantarotto, D.; Briand, J. P.; Muller, S. Cellular uptake of functionalised carbon nanotubes is independent of functional group and cell type. *Nat. Nano* **2007**, *2*, 108–113.

24. Keston, A. S.; Brandt, R. The fluorometric analysis of ultramicro quantities of hydrogen peroxide. *Anal. Biochem.* **1965**, *11*, 1–5.

25. Nel, A. E.; Mädler, L.; Velegol, D.; Xia, T.; Hoek, E. M. V.; Somasundaran, P.; Klaessig, F.; Castranova, V.; Thompson, M. Understanding biophysicochemical interactions at the nano-bio interface. *Nat. Mater.* **2009**, *8*, 543–557.

26. Kam, N. W. S.; Liu, Z. A.; Dai, H. J. Carbon nanotubes as intracellular transporters for proteins and DNA: an

investigation of the uptake mechanism and pathway. *Angew. Chem., Int. Ed.* **2006**, *45*, 577–581.

27. Nel, A.; Xia, T.; Madler, L.; Li, N. Toxic potential of materials at the nanolevel. *Science* **2006**, *311*, 622–627.

28. Jia, G.; Wang, H. F.; Yan, L.; Wang, X.; Pei, R. J.; Yan, T.; Zhao, Y. L.; Guo, X. B. Cytotoxicity of carbon nanomaterials: single-wall nanotube, multi-wall nanotube, and fullerene. *Environ. Sci. Technol.* **2005**, *39*, 1378–1383.

29. Fiorito, S.; Serafino, A.; Andreola, F.; Bernier, P. Effects of fullerenes and single-wall carbon nanotubes on murine and human macrophages. *Carbon* **2006**, *44*, 1100–1105.

30. Zhang, D. W.; Yi, C. Q.; Zhang, J. C.; Chen, Y.; Yao, X. S.; Yang, M. S. The effects of carbon nanotubes on the proliferation and differentiation of primary osteoblasts. *Nanotechnology* **2007**, *18*, 475102.

31. Wörle-Knirsch, J. M.; Pulskamp, K.; Krug, H. F. Ooops they did it again! Carbon nanotubes hoax scientists in viability assay. *Nano Lett.* **2006**, *6*, 1261–1268.

32. Porter, A. E.; Gass, M.; Bendall, J. S.; Muller, K.; Goode, A.; Skepper, J. N.; Midgley, P. A.; Welland, M. Uptake of noncytotoxic acid-treated single-walled carbon nanotubes into the cytoplasm of human macrophage cells. *ACS Nano* **2009**, *3*, 1485–1492.

33. Lovat, V.; Pantarotto, D.; Lagostena, L.; Cacciari, B.; Grandolfo, M.; Righi, M.; Spalluto, G.; Prato, M.; Ballerini, L. Carbon nanotube substrates boost neuronal electrical signaling. *Nano Lett.* **2005**, *5*, 1107–1110.

34. Correa-Duarte, M. A.; Wagner, N.; Rojas-Chapana, J.; Morsczeck, C.; Thie, M.; Giersig, M. Fabrication and biocompatibility of carbon nanotube-based 3D networks as scaffolds for cell seeding and growth. *Nano Lett.* **2004**, *4*, 2233–2236.

35. Firkowska, I.; Godehardt, E.; Giersig, M. Interaction between human osteoblast cells and inorganic two-dimensional scaffolds based on multiwalled carbon nanotubes: a quantitative AFM study. *Adv. Funct. Mater.* **2008**, *18*, 3765–3771.

36. Gaillard, C.; Cellot, G.; Li, S. P.; Toma, F. M.; Dumortier, H.; Spalluto, G.; Cacciari, B.; Prato, M.; Ballerini, L.; Bianco, A. Carbon nanotubes carrying cell-adhesion peptides do not interfere with neuronal functionality. *Adv. Mater.* **2009**, *21*, 2903–2906.

37. Wu, P.; Chen, X.; Hu, N.; Tam, U. C.; Blixt, O.; Zettl, A.; Bertozzi, C. R. Biocompatible carbon nanotubes generated by functionalization with glycodendrimers. *Angew. Chem., Int. Ed.* **2008**, *47*, 5022–5025.

38. Park, S. Y.; Park, S. Y.; Namgung, S.; Kim, B.; Im, J.; Kim, Y.; Sun, K.; Lee, K. B.; Nam, J. M.; Park, Y.; Hong, S. Carbon nanotube monolayer patterns for directed growth of mesenchymal stem cells. *Adv. Mater.* **2007**, *19*, 2530–2534.

39. Tay, C. Y.; Gu, H. G.; Leong, W. S.; Yu, H. Y.; Li, H. Q.; Heng, B. C.; Tantang, H.; Loo, S. C. J.; Li, L. J.; Tan, L. P. Cellular behavior of human mesenchymal stem cells cultured on single-walled carbon nanotube film. *Carbon* **2010**, *48*, 1095–1104.

40. White, M. A.; Anderson, R. G. W. Signaling networks in living cells. *Annu. Rev. Pharmacol. Toxicol.* **2005**, *45*, 587–603.

41. Kaur, G.; Valarmathi, M. T.; Potts, J. D.; Wang, Q. The promotion of osteoblastic differentiation of rat bone marrow stromal cells by a polyvalent plant mosaic virus. *Biomaterials* **2008**, *29*, 4074–4081.

42. Manna, S. K.; Sarkar, S.; Barr, J.; Wise, K.; Barrera, E. V.; Jejelowo, O.; Rice-Fich, A. C.; Ramesh, G. T. Single-walled carbon nanotube induces oxidative stress and activates nuclear transcription factor kappa B in human keratinocytes. *Nano Lett.* **2005**, *5*, 1676–1684.

43. Kagan, V. E.; Tyurina, Y. Y.; Tyurin, V. A.; Konduru, N. V.; Potapovich, A. I.; Osipov, A. N.; Kisin, E. R.; Schwegler-Berry, D.; Mercer, R.; Castranova, V.; Shvedova, A. A. Direct and indirect effects of single walled carbon nanotubes on RAW 264.7 macrophages: role of iron. *Toxicol. Lett.* **2006**, *165*, 88–100.

44. Ryoo, H. M.; Lee, M. H.; Kim, Y. J. Critical molecular switches involved in BMP-2-induced osteogenic differentiation of mesenchymal cells. *Gene* **2006**, *366*, 51–57.

45. Korchynskyi, O.; ten Dijke, P. Identification and functional characterization of distinct critically important bone morphogenetic protein-specific response elements in the Id1 promoter. *J. Biol. Chem.* **2002**, *277*, 4883–4891.

46. Komori, T. Requisite roles of Runx2 and Cbfb in skeletal development. *J. Bone Miner. Metab.* **2003**, *21*, 193–197.

47. Benoit, D. S. W.; Collins, S. D.; Anseth, K. S. Multifunctional hydrogels that promote osteogenic human mesenchymal stem cell differentiation through stimulation and sequestering of bone morphogenic protein 2. *Adv. Funct. Mater.* **2007**, *17*, 2085–2093.

48. Sengupta, P.; Xu, Y.; Wang, L.; Widom, R.; Smith, B. D. Collagen α1(I) gene (*COL1A1*) is repressed by RFX family. *J. Biol. Chem.* **2005**, *280*, 21004–21014.

49. Zhang, W. X.; Yang, N. L.; Shi, X. M. Regulation of mesenchymal stem cell osteogenic differentiation by glucocorticoid-induced leucine zipper (GILZ). *J. Biol. Chem.* **2008**, *283*, 4723–4729.

50. Kelly, K. A.; Gimble, J. M. 1,25-Dihydroxy vitamin D_3 inhibits adipocyte differentiation and gene expression in murine bone marrow stromal cell clones and primary cultures. *Endocrinology* **1998**, *139*, 2622–2628.

51. Gori, F.; Divieti, P.; Demay, M. Cloning and characterization of a novel WD-40 repeat protein that dramatically accelerates osteoblastic differentiation. *J. Biol. Chem.* **2001**, *276*, 46515–46522.

52. Qi, S. J.; Yi, C. Q.; Chen, W. W.; Fong, C. C.; Lee, S. T.; Yang, M. S. Effects of silicon nanowires on HepG2 cell adhesion and spreading. *ChemBioChem.* **2007**, *8*, 1115–1118.

53. Qi, S. J.; Yi, C. Q.; Fong, C. C.; Ji, S. L.; Yang, M. S. Cell adhesion and spreading behavior on vertically aligned silicon nanowire array. *ACS Appl. Mater. Interfaces* **2009**, *1*, 30–34.

ARTICLE